

Computational Simulation of Flow over a Cylinder in Ground Effect, Using PANS

M. Nirooei^{*1}, M. Salimi², M. Taeibi-Rahni², M. Mahdavianesh¹

¹Department of Mechanical Engineering, Neyriz Branch, Islamic Azad University, Neyriz, Iran

²Department of Aerospace Engineering, Sharif University of Technology, Tehran, Iran
m.nirooei@gmail.com; mrsalimi@sharif.ac.ir; taeibi@sharif.edu; mmmahdavianesh@gmail.com

Abstract: Recently, Very Large Eddy Simulation approach has attracted a great deal of attention among researchers. This approach can be thought of as an intermediate approach in flow field filtering view point compared with Direct Numerical Simulation and Reynolds-Averaged Navier-Stokes. One famous method to this approach is Partially Averaged Navier-Stokes. Early studies have demonstrated the capability of this technique in flow prediction; however, this method still needs to be evaluated under more flow conditions to ensure its reliable performance. In this study, the performance of PANS $k-\omega$ method in the simulation of turbulent flow around a cylinder with square cross section close to a flat surface, and at Reynolds number of 13200, has been evaluated. Flow around a cylinder provides a good criterion to assess capabilities of the proposed method. To do so, three different filters have been evaluated dynamically and compared with each other and Wilcox $k-\omega$ model. Results indicate that at such a Reynolds number, method is as accurate as $k-\omega$ method.

[M. Nirooei, M. Salimi, M. Taeibi-Rahni, M. Mahdavianesh. **Computational Simulation of Flow over a Cylinder in Ground Effect, Using PANS.** *Life Sci J* 2013;10(8s):195-202] (ISSN:1097-8135).
<http://www.lifesciencesite.com>. 27

Keywords: Very large eddy simulation; PANS method, Wilcox model; Turbulent flow

1. Introduction

The Very Large Eddy Simulation (VLES) has been widely utilized. On the one hand, these methods are similar to the LES approach, and on the other hand, they are similar to the RANS methods. Since these methods use the transport equations of the RANS approach, they are similar to RANS; and since they are able to capture the turbulent flow structures, they resemble the LES. In other words, this method tries to keep the adequate performance of the RANS approach from the computation perspective (computation time and cost) while offering the capability of solving turbulent flow structures, which exists in the Large Eddy Simulation approach. Figure 1 shows the comparison between the performances of RANS, LES and VLES approaches in the energy spectrum. The VLES approach has different methodologies; however all of them have the following common characteristics:

- In contrast to RANS approach in which the flow field is decomposed into average and fluctuating components, in all of these methods, the flow field is decomposed into the solved and unresolved components.
- Decomposition caused insertion of unknown terms into the equations (similar to Reynolds stress in the RANS approach). These unknowns should be modeled in order to set up

the equations; consequently other transport equations are introduced and added to the set of Navier-Stokes equations (at least two equations). It should be noted that this approach is different from the LES in which the grid-size determines the unresolved scales.

- Although all the considered transport equations for the formulation of the unknown terms appearing in the equations are based on the RANS approach, these equations are not the exact equivalents of RANS equations, and they are sensitive to the decomposition of the flow field into the solved and unresolved portions.

- The equations are formulated in such a way that under certain conditions, these methods act exactly as the RANS or the DNS approach. In fact, these methods can be considered as a bridge between the RANS and DNS approaches (Gerolymos, et al., 2006).

Of the different existing methods, the Partially Averaged Navier-Stokes (PANS) model has attracted more interest. This technique has been presented by Girimaji et al. (2003). Their work is based on solving a percentage of the kinetic energy spectrum of the turbulent flow and modeling the remaining portion of the flow. To specify the solved part of the flow's kinetic energy, control parameter f_k has been introduced, which represents the ratio of the modeled kinetic energy to total kinetic energy of the turbulent

flow. This parameter adopts constant values between 0 and 1 for the whole flow; so that if $f_k = 0$, the model acts exactly according to the DNS method, and if $f_k = 1$, the model behaves like the RANS approach. Therefore, the PANS model is a bridge between the RANS and DNS approaches. To simulate the unresolved portion of flow, Girimaji et al. used the standard $k-\epsilon$ model with coefficients adapted to the PANS method; while Lakshmipathy and Girimaji (2006) employed the Wilcox $k-\omega$ model with coefficients adapted to the PANS method in order to model the eddy viscosity of the unresolved flow portion. Instead of assigning a constant number to f_k , Elmiligui et al. (2010) used a damping function which depends on the turbulence length scale and grid size. This function is updated at each time step and in every cell, and takes on values between 0 and 1. There are many examples of objects situated near flat surfaces, such as suspension bridges, oil pipes which are laid on ocean beds, and chimneys near walls. A body exposed to a uniform stream, away from a wall, causes opposite circulation vortices which alternatively shed into the wake from both up and down of the body. These vortices apply aerodynamic forces to the object and they also increase the fluid mixing in the wake. When the object is brought close to a flat surface, the vortex shedding characteristics and thus the transport phenomena in the wake are totally affected (Shi, et al., 2010). Although a cylinder has a simple form, the flow around it is very complex, and various types of phenomena such as flow separation, vortex shedding and transition to turbulent flow can be observed in it. Principally, low-Reynolds turbulent flows constitute a challenge for the VLES approach. In this Study, the ability of PANS $k-\omega$ method in solving this type of flow has been investigated and also performance of three different control parameters in the PANS $k-\omega$ method, under the ground effect, has been analyzed dynamically.

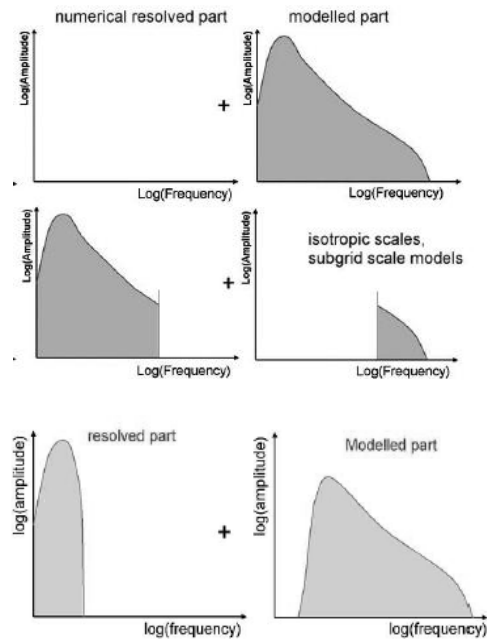


Figure 1. Comparison between performances of RANS, LES and VLES approaches (top to bottom) in the energy spectrum (Ogor, 2006)

2. Governing equations

In this issue, the incompressible Navier-Stokes equations have been used:

$$\frac{\partial V_i}{\partial x_i} = 0, \tag{1}$$

$$\frac{\partial V_i}{\partial t} + V_j \frac{\partial V_i}{\partial x_j} = -\frac{\partial p}{\partial x_i} + \nu \frac{\partial^2 V_i}{\partial x_j \partial x_j}. \tag{2}$$

Contrary to the RANS approach, in which velocity is split into the mean and fluctuating parts, the flow field in the PANS approach is divided into the following solved and unresolved (modeled) sections:

$$V_i = U_i + v'_i, \tag{3}$$

$$p = P + p_u,$$

Where, v'_i is the unresolved velocity, U_i is the solved velocity, p is the solved pressure and p_u is the unresolved pressure. The cutoff (designating the boundary between the solved and unresolved sections) can be arbitrary. With the application of the filter, we get: $\langle V_i \rangle = U_i$, and $\langle p_i \rangle = P$. By

filtering Eq. (1) and (2), the filtered Navier-Stokes (PANS) equations are obtained as follows:

$$\frac{\partial U_i}{\partial x_i} = 0, \tag{4}$$

$$\frac{\partial U_i}{\partial t} + \frac{\partial \langle V_k V_i \rangle}{\partial x_k} = -\frac{\partial P}{\partial x_i} + \nu \frac{\partial^2 U_i}{\partial x_k \partial x_k}, \tag{5}$$

Term $\langle V_i V_j \rangle$, which is unknown, has been added to the equations. This term can be calculated as follows (similar to Reynolds stresses in the RANS approach):

$$\tau(f, g) = \langle fg \rangle - \langle f \rangle \langle g \rangle,$$

$$\tau(f, g, h) = \langle fgh \rangle - \langle f \rangle \tau(g, h) - \tag{6}$$

$$\langle g \rangle \tau(f, h) - \langle h \rangle \tau(f, g) - \langle f \rangle \langle g \rangle \langle h \rangle,$$

Where, g, f, and h are arbitrary variables. By performing mathematical operations similar to those in the RANS method, the general form of the unresolved kinetic energy equation is obtained:

$$\frac{\partial k}{\partial t} + U_j \frac{\partial k}{\partial x_j} = p - \varepsilon - T, \tag{7}$$

$$P = \frac{1}{2} \tau(V_i, V_j) \frac{\partial U_i}{\partial x_j}, \quad \varepsilon = \nu \tau\left(\frac{\partial V_i}{\partial x_j}, \frac{\partial V_i}{\partial x_j}\right), \quad \text{and}$$

$$k = \frac{1}{2} \tau(V_i, V_j).$$

T is the transport term. In the PANS method, by using the Boussinesq approximation, the term equivalent to Reynolds stress can be related to the solved velocity field. Thus, to set up the equations, it will be necessary to add two transport equations to the Navier-Stokes equations. The Boussinesq hypothesis is expressed as:

$$\tau(V_i V_j) = -\nu S_{ij} + \frac{2}{3} k S_{ij}. \tag{8}$$

To close the equations, it is necessary to know the values of k and ν in the Boussinesq relationship. The RANS approach can be used to formulate the PANS equations. The aim is setting up the equations in such a way that the PANS model becomes a bridge between the RANS and DNS approaches. This can be achieved by revising the RANS equations' coefficients. These coefficients should be compatible with the filter (control

parameter) applied by the user. The relationship between the eddy viscosities of PANS and RANS methods should be investigated. Considering the applied filter, gives:

$$\nu_u = \frac{k_u}{\beta^* \omega_u} = \frac{k f_k}{\beta^* \omega f_\omega} = \frac{f_k}{f_\omega} \nu_t. \tag{9}$$

As can be seen, no change has been made to β^* coefficient. It should be mentioned that, presently, there is no guarantee as to the optimality of this coefficient, and that it is necessary to conduct more studies on this subject. By applying this filter to the Wilcox $k-\omega$ equations, the equations are modified as follows (Lakshminpathy and Girimaji, 2006):

$$\frac{\partial k}{\partial t} + u_j \frac{\partial k}{\partial x_j} = p - \beta^* k \omega + \frac{\partial}{\partial x_j} [(v + \sigma v_t) \frac{\partial k}{\partial x_j}], \tag{10}$$

$$\frac{\partial \omega}{\partial t} + u_j \frac{\partial \omega}{\partial x_j} = \alpha \frac{\omega}{k} p - \beta k \omega^2 + \frac{\partial}{\partial x_j} [(v + \sigma v_t) \frac{\partial \omega}{\partial x_j}], \tag{11}$$

$$\beta^* = 0.09, \quad \alpha = 5/9, \quad \beta = 3/40, \quad \sigma = 0.5, \quad \text{and}$$

$$\beta = \alpha \beta^* - f_k (\alpha \beta^* - \beta).$$

It is obvious that if $f_k = 1$, it will be the same as Wilcox $k-\omega$ model.

3. Selection of control parameter and solution algorithm

In this study, four different control parameters are compared. First case, $f_k = 1$. Second case, the damping function presented by Nichols and Nelson (2003) for a hybrid RANS/LES method has been used as follows:

$$f_k = \{1 + \tanh(2\pi(\Lambda - 0.5))\} / 2,$$

$$l_u = \frac{k^{1/2}}{\beta^* \omega}, \quad \lambda = \frac{l_u}{\Delta}, \quad \Delta = \max(\Delta x, \Delta y, \Delta z), \quad \Lambda = \frac{1}{1 + \lambda^{4/3}}, \tag{12}$$

Third case, to obtain the control parameter, reasoning similar to that of Kolmogorov has been used. First, it is necessary to define parameter f_ω as (Song and Park, 2009):

$$f_\omega = \frac{\omega}{\omega_u} \tag{13}$$

In the above relation, ω_u is unresolved turbulent frequency. If it is assumed that the smallest solved

scale (η_r) is determined by dissipation and eddy viscosity, can be written:

$$\eta_r \sim \left(\frac{v_u^3}{\beta^* \omega_u k_u} \right)^{1/4}, \quad (14)$$

Considering the definition for eddy viscosity and control parameters, this can be written:

$$v_u = \frac{k_u}{\omega_u} = \frac{f_k k}{f_\omega \omega}. \quad (15)$$

By inserting the above relation into Eq. (14) and

considering that $f_\omega = \frac{1}{f_k}$, the following relation can be easily obtained:

$$\eta_r = \frac{\left(\frac{f_k k}{f_\omega \omega} \right)^{3/4}}{\left(\beta^* \omega_u^* k f_k \right)^{1/4}} = \beta^{*3/4} f_k^{3/2} l, \text{ Where } l = \frac{k^{1/2}}{\beta^* \omega} \quad (16)$$

As was expected, the smallest solved scale in the PANS method is dependent on f_k and the turbulence scale. Similar to the DNS approach (in which the grid size should have the same order as the Kolmogorov scale), can be mentioned:

$$\eta_r = \beta^{*3/4} f_k^{3/2} l \sim \Delta, \quad (17)$$

Therefore, the final relation is as follows:

$$f_k = \frac{1}{\sqrt{\beta^*}} \left(\frac{\Delta}{l} \right)^{2/3}. \quad (18)$$

Fourth case, since in the previous section it was shown that $f_k \propto \left(\frac{\Delta}{l} \right)^{2/3}$, the following equation is

used to estimate the value of f_k :

$$f_k = \left(\frac{\Delta}{l} \right)^{2/3}. \quad (19)$$

To estimate f_k , total kinetic energy and dissipation should be specified. However, these values are not known before solving the problem. To resolve this problem, different algorithms can be presented. In this research, to achieve an appropriate distribution of f_k , the problem was first solved through the RANS approach (although not necessarily with a high accuracy), and then using the obtained results, the value of f_k was

estimated in the computational domain. Hence, this algorithm can be executed in the following five steps:

- First, a computational grid is generated for the considered problem and then by using the RANS approach, the problem is initially solved.
- By means of the information obtained from the RANS solution, the turbulence length scales are calculated.
- The distribution of f_k is estimated through relations (Eq. (12), (18) and 19).
- When the value of f_k is determined, the PANS method can be used to solve the problem.
- Finally, f_k is updated by using information obtained from previous step at the every time step.

4. Numerical methodology

In the present investigation, the governing equations in the 3D state have been converted to linear algebraic equations by the finite volume method, on a non-uniformly structured and staggered grid. The transient algorithm of SIMPLE has been used to establish the relationship between the velocity and pressure fields; and for time discretization, the fully implicit method with first-order accuracy has been employed. Also, the Van Leer method has been used for space discretization (Van Leer, 1974). Except at the maximum and minimum points, this method is accurate to the second order.

Because a higher gradient exists near the cylinder, especially at the corners and between the flat surface and cylinder, in order to reduce computation cost and achieve a better accuracy, the grid has been clustered. Figure 2 shows a view of the grid which is used in this research.

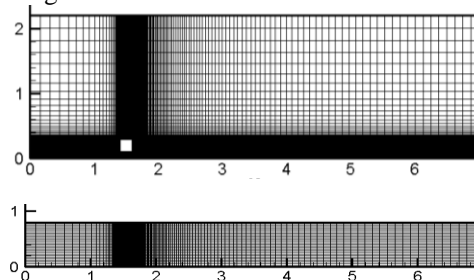


Figure 2. The grid which is used in the present research

Figure 3 shows the applied boundary conditions. Since the upper boundary has an adequate distance from the cylinder, the perpendicular component of velocity on it can be considered as

zero. Along the z-axis, the periodic condition has been applied.

Boundary condition at no-slip surfaces are given by the following relationships (Bardina, et al., 1997)

$$k = 0, \omega = \frac{60}{\beta y^2}, \tag{20}$$

Where, y is the distance of the nearest point to the wall.

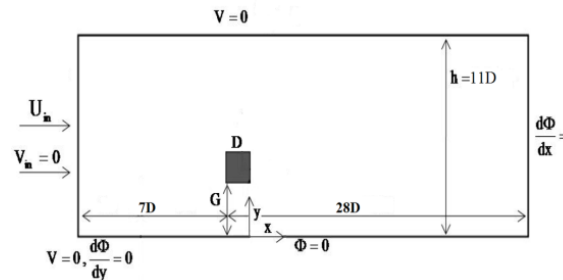


Figure 3. Geometry and boundary conditions of the present research

5. Results

In this research, the flow around a cylinder with square cross section, and located near a flat surface, has been investigated. The dimensionless cylinder-to-surface distance is $\frac{G}{D} = 0.5$. The

dimensionless boundary layer thickness at the location of the cylinder (before installing the cylinder) is $\frac{\delta}{D} = 0.75$. The flow's inlet velocity

is $U_0 = 10 \text{ m/s}$, and the Reynolds number based on the inlet free-stream velocity and cylinder width is 13,200. For inlet flow, a velocity profile

that satisfies the condition of $\frac{\delta}{D} = 0.75$ at the

location of the cylinder (before installing the cylinder) has been used (Figure 4).

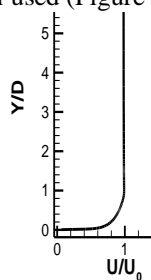


Figure 4. Inlet velocity profile

The experimental findings of Shi et al. (2010) showed that with the cylinder getting closer to the

surface, the symmetry of the flow field is lost and the near-wall vortices become weaker and more stretched, while the vortices above the cylinder form and shed at higher position. The flow above the cylinder is very similar to the case where the cylinder was away from the wall. Flow at the leading edge of the cylinder undergoes separation and no longer attaches to the cylinder; this causes a recirculation region to be formed over the cylinder. On the other hand, below the cylinder, the flow at the leading edge gets separated, but attaches again to the cylinder surface.

In this section, the performances of control parameters have been compared to each other. Figure 5 illustrates the streamwise velocity profile at various cross sections. At the two cross sections of $x/D = 1.25, 0.25$, where the flow separates over the cylinder, all the methods display an identical performance. Also in the lower section of the cylinder (experimental results are not available), all the mentioned procedures have predicted almost identical profiles. These profiles and Figure 6 indicate that below the cylinder, flow gets separated from the cylinder and attaches again to cylinder surface. At the two cross sections of $x/D = 1.25, 0.25$, all the methods have predicted the separation of the flow as it expands when passing through the wall-cylinder gap, which is the result of boundary layer thickening at these cross sections; however, the experimental results don't confirm such findings. Results show that the first and third cases are more accurate than the other cases. By moving away from the cylinder, the results of second and fourth cases become more exact. For near-wall flows, the second case performs a little better than the fourth case.

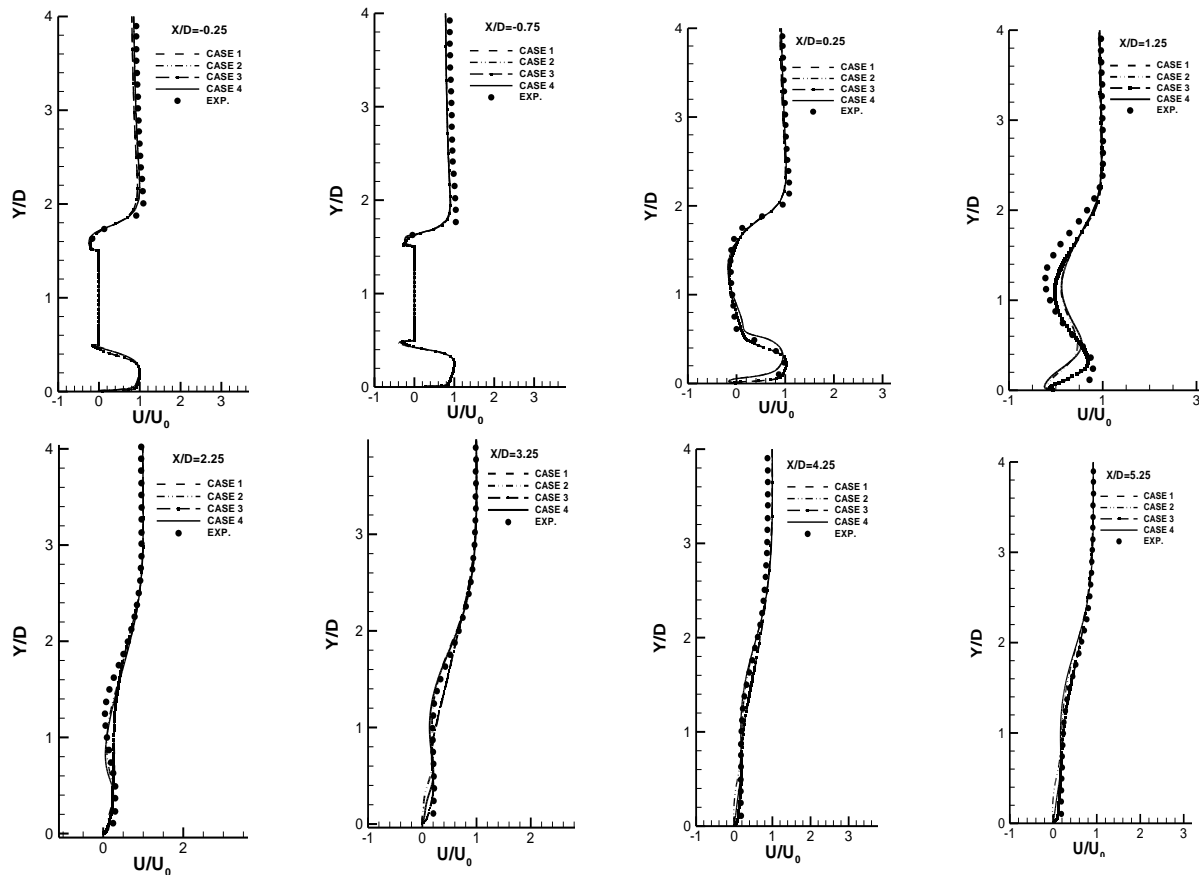


Figure 5. Streamwise velocity profile at various cross sections in comparison with the experimental results (Shi et al., 2010)

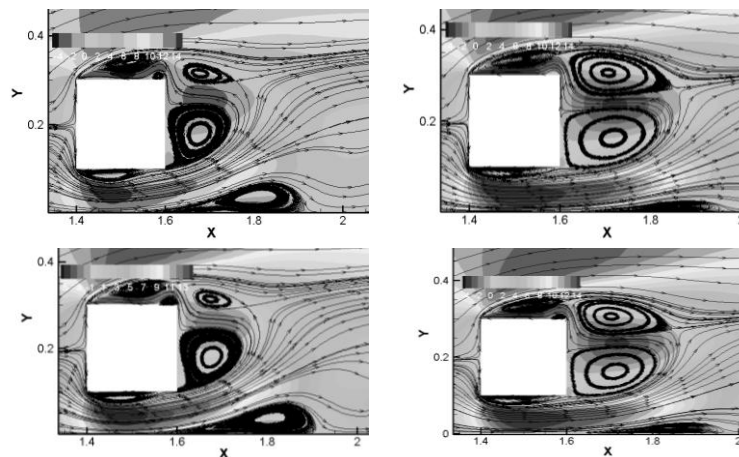


Figure 6. Streamwise velocity contours, from right to left: PANS method; first case; second case; third case; fourth case

At the last cross sections, the results of the first and third cases have a better agreement with the experimental results. Due to the decrease of flow gradients, all the methods exhibit a good correlation with the experimental results at the last cross sections. Because the near-cylinder flow

is of more importance and both the first and third cases predict a more accurate separation region, it can be said that in general, the first and third cases enjoy a higher accuracy than the other cases. In view of Figure 7, it is clear that the control parameter distribution in the third case, contrary

to the second and fourth cases, doesn't have high gradients in the solution domain. The most important point in this figure is that in the near-wall region, the control parameter value is one. This means that in this method, any type of wall function in the log-law area can be used.

The question here is that, why in this problem, the PANS method could not provide more accurate results, as expected. To answer this question, first we need to recall the Kolmogorov's third similarity hypothesis. Figure 8 shows the energy spectrum for two high-Reynolds and low-Reynolds cases nondimensionalized by Kolmogorov scales. The dissipation ranges for both Reynolds numbers are identical; while for the low Reynolds numbers, the inertial range is not extensive as in the higher Reynolds number case. The studied problem in the present research also has a relatively low Reynolds number; therefore, the overlap area between energy containing range and dissipation range is more, which makes it difficult to achieve an appropriate distribution of the control parameter (Lakshmipathy, 2004)

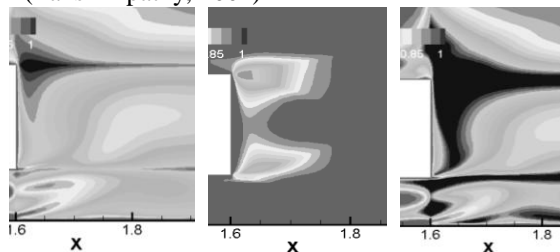


Figure 7. Control parameter distribution contours (from right to left): second case, third case; fourth case

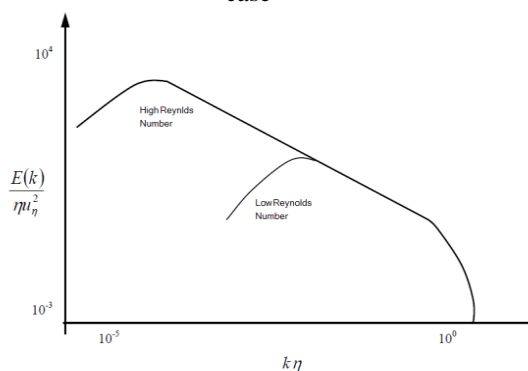


Figure 8. Energy spectrum for different Reynolds numbers (Lakshmipathy, 2004)

6. Conclusion

In all the mentioned methods, this leads to the formation of a separation zone on the lower wall, in the expansion region of flow exiting through

the cylinder-surface gap; while previous experimental works haven't reported the existence of such a phenomenon at this cylinder-to-surface distance ($G/D = 0.5$). When a less-than-sufficient value is chosen for the control parameter, which in this method is equivalent to the wave number in the LES, the vortices are estimated smaller than their real size (underestimated). According to the results of this research, because the Reynolds number was not high enough in this problem, the PANS $k-\omega$ method was able to achieve the RANS results at the most. The results indicate that at low Reynolds numbers, the third control parameter predicts the best results. Therefore, this method is applicable to flows with a high enough Reynolds number provided that a distinct separation scales can be delineated between the energy-containing range and the dissipation range. Otherwise, the proper estimation of the control parameter in the solution domain becomes difficult, and we may have to go back to the RANS approach.

References

1. Bardina, J.E., Huang, P.G., Coakley, and T.J. (1997): Turbulence Modeling Validation, Testing, and Development, NASA TM 110446.
2. Elimilgui, A., Abdol-Hamid, k., and Paul, P.s. (2010): Numerical Study of Flow Past Circular Cylinder Using Hybrid Turbulence Formulations, Journal of Aircraft, Vol. 47, No. 2: 434-440.
3. Gerolymos, G., Vallet, I., and Senechal, D. (2006): Reynolds-Stress-Model-VLES Multiblock Implicit Solver using High-Order Upwind Schemes, 36th, AIAA Fluid Dynamics Conference and Exhibit, 5-8 June, San Francisco, California.
4. Girimaji, S., and Sreenivasan, R. (2003): PANS Turbulence Model for Seamless Transition between RANS, LES: Fixed-Point Analysis and Preliminary Results, ASME 4th, Joint Fluids Summer Engineering Conference, July 6-10, Honolulu, Hawaii, USA.
5. Lakshmipathy, S., and Girimaji, S. (2006): Partially Averaged Navier Stokes Method for Turbulent Flow: $k-\omega$ Model Implementation, 44th, AIAA Aerospace

- Sciences Meeting and Exhibit, Reno, Nevada, January 9-12.
6. Lakshmipathy, S. (2004): PANS Method for Turbulence: Simulations of High and Low Reynolds Number Flows Past a Circular Cylinder, M.Sc. Thesis, Texas A&M University, Aerospace Engineering Dept.
 7. Nichols, R.H., and Nelson, C.C. (2003): Application of Hybrid RANS/LES Turbulence Models, 41st, Aerospace Sciences Meeting and Exhibit, Reno, Nevada 6-9 January.
 8. Ogor, B.I., Gyllenram, W., Ohlberg E., Nilsson H., and Ruprecht A. (2006): An Adaptive Turbulence Model for Swirling Flow, Conference on Turbulence and Interactions, Porquerolles, France, May 29-June 2.
 9. Shi, L.L., Liu, Z.Y., and Sung, H.J. (2010): On the Wake With and Without Vortex Shedding Suppression Behind a Two Dimensional Square Cylinder in Proximity to a Plane Wall, Journal of Wind Engineering Industrial Aerodynamics, Vol. 98, No. 10: 492-503.
 10. Song, C.S., and Park, S.O. (2009): Numerical Simulation of Flow Past a Square Cylinder Using Partially-Averaged Navier–Stokes Model, Journal of Wind Engineering and Industrial Aerodynamics, Vol. 97, No. 1: 37-47.
 11. Van Leer, B. (1974): Towards the ultimate conservative difference scheme II. Monotonicity and conservation combined in a second order scheme, J. Comp. Phys. 14 (4): 361–370.

4/2/2013